

Problems in image target-based color correction

Gabriele Simone¹, Marco Gaiani², Andrea Ballabeni², Alessandro Rizzi¹

¹MIPS Lab - Computer Science Department - University of Milan, Italy.

²Department of Architecture – Alma Mater Studiorum University of Bologna, Italy.

Abstract

This paper aims at presenting some problems that everyone could experience in the process of image target-based color correction (CC). We have acquired a set of images using a color checker, here we present some measures of these image before and after the color correction and we compare them with the actual values of the color checker. Comments about the results and their departures from the scene are reported together with the changes after color correction. It is shown how real scene acquisitions are subject to many issues that makes color correction process very far from the idealized colorimetric ideas.

Introduction

To achieve an accurate color description and reproduction using images a key point is the determination of chromatic and tonal properties using the device dependent RGB pixel values of the image. The classic colorimetric approach focuses on the spectral responses of the color channels, even if in general, do not match those of the CIE Standard Colorimetric Observer. Information about the correspondence between the RGB values produced by the camera and the image irradiances is not generally available to users but it is essential for reproduction. The problem consists in recovering a relationship between the irradiance values and the pixel encoding produced by the camera. This step is referred as ‘camera characterization’ (CC). CC techniques in the literature are divided into two general groups: spectral sensitivity-based and color target-based approaches, as specified by ISO17321 [1].

Spectral sensitivity-based methods connect device-dependent and device-independent color spaces by a combination of camera spectral sensitivity curves and color matching functions. Although their approach is interesting from the physical point of view, their applicability on actual scenes is usually difficult.

The target-based characterization methods establish the color relationship from camera digits to a set of color patches with available pre-measured spectral or colorimetric data. Target-based characterization methods are usually intended for a lighting geometry, color target materials, and a specific surface structure. The most accurate target-based CC requires to record its output for all possible lighting and exposure and comparing it with separately measured values for the same lighting and exposure conditions [2]. However, this process generates a massive and unmanageable amount of data. Therefore, the device response is measured only for a selected set of stimuli, according to the capturing settings and the scene features.

Despite these problems target-based CC are the most popular technique in many fields of the photography as fashion, heritage, architecture, archaeology, portraiture, furniture design, interior design etc. essentially due to its flexibility and easy to use. It involves a simple capture of an inexpensive, standard color pattern, is well rooted in the ICC color management workflows, and exploit commercial or open-source automatic software as the Calibrite ColorChecker Camera Calibration [3].

Following a theoretical approach, one could think that correcting color in an image can be seen as finding a kind of unique shift in a well-ordered series of color difference among patches. From this perspective the problem to be solved is that of the mathematical shape of the transformation to map device-dependent and device-independent spaces with adequate performance. This has led to the development of many forms of solutions: linear transformations, multidimensional lookup tables, least-squares polynomial regressions, and others) [4].

However real implementations are very far from the above illustrated ideal situation. Many different factors form a long list of potential departures from the value of the scene to acquire, to the point that the many patches of a target inserted in the scene for color correction have a sort of chaotic range of color shift vectors. It is well known that differences in vector direction make the color shift more visible and annoying [5].

Moreover, these distortions need to be added to the inaccuracies typical of the operator errors in the capture process and the problem related to camera orientation with respect to the target and the lighting sources, as well surveyed by [6]. In addition, other problems can be the color cast appearing in the case of environment with surrounding walls or large objects with saturated colors, sensor blooming, saturation, gamut inaccuracies, etc.

As last item of this long list of potential problems we want to underline the lens glare. Usually not considered it is a huge source of departures from the value acquired at a point to the actual corresponding value in the scene.

All the departures from the theoretical value of acquisition generated by these phenomena, makes the target-based color correction an interpolation issue, where the practical impossibility of linear coherent shifts gives importance to the minimization of vectorial color differences.

In this paper we present a general ‘panorama’ to show that the problems mainly affecting the results of CC are a wider range than the usually studied problems (i.e., the target selection, and the evaluation of the selected formula to determine the goodness of the CC operation, precision of color differences, etc.) and that the today studies aiming to solve target-based problems address residual factors.

We investigate and shows results about six class of problems:

1. Selection of the formula to determine the goodness of the CC operation
2. Color patches importance in the CC process
3. Exposure correctness in the acquired image
4. Uniformity of the illumination on the target image
5. Glare effects
6. Noise effects
7. Use of different output color space.

We exploit examples of real-world acquisitions showing the above-described problems. We used a color correction technique called SHAFT (SAT & HUE Adaptive Fine Tuning) [7], an automated

framework for target-based CC. The software is designed to minimize possible problems in target-based CC.

The CC SHAFT technique

SHAFT is a software for target-based CC supported by libRAW, a cross-platform open-source RAW image processing program [8] to which are entrusted the operations of demosaicking, devignetting, and white balance. SHAFT is based on the CC linear approach by Bruce Fraser, the so-called Adobe Camera Raw (ACR) calibration scripts for calibration by iterative approximations. As target are admitted the Calibrite ColorChecker Classic (XCC), the most common solution for the CC with 24 standardized patches with known reflectance and its smaller version Passport, and the Digital SG ColorChecker. The software differs from the original technique for the number and the types of tests done along the processing pipeline and for the algorithm used to find the best variation from the original values of the selected parameters (exposure, contrast, white balance, hue, and saturation on each RGB channel). SHAFT is completely automated, exploit previously proposed solutions for the target recognition on the image and is written in MATLAB to avoid the use of Adobe Photoshop. To limit its main problem (i.e., failure of the CC process for original highly incorrect images with high chromaticity) SHAFT is coupled with a polynomial regression correction based on least squares fitting [9].

In our pipeline, to avoid uncontrolled modification of the RAW pixel intensity values, in-camera processing retained only the basic operations: bad pixel removal, dark frame, bias subtraction, green channel equilibrium correction, Bayer interpolation. The off-camera workflow is as follows:

- RAW image 16-bit linearization and devignetting
- Image denoise
- Color target detection
- Exposure equalization and white balance
- Polynomial function for CC
- Image CC using the new fitting function
- SHAFT CC
- Image color rendition using the selected color space.

In detail, white balance was performed on the patch D4 of the XCC (Fig.1), performing a simple von Kries-type transformation. Consequently, as a white point the D65 illuminant was selected in XYZ space.

Obviously, SHAFT improve over a traditional ‘manual’ CC. In Fig.2 are reported results of a ‘manual’ CC against a SHAFT-based CC on three selected images to see how it compares colorimetrically to the reference and the SHAFT processing.

Experimental setup and tests description

For the experiment our dataset of 22 XCC RAW images described in [10] was used (Fig. 3). The dataset consists of images captured in photo studio, indoor, architectural scenarios, and outdoor environment, where natural light characteristics are extremely complex and changeable and represent different cases and problems of target-based CC. These targets present many types of distortions typical of the real scene capture, but in the dataset, there are also target captured in a photo studio environment using professional cameras.

As final rendered color space we used the Apple Display P3, a variant of the DCI-P3 color space with D65 illuminant. It minimizes most part of the downsides of the sRGB color space the today most used [11]. The Display P3 is 25% larger than the tiny sRGB color space. It is supported by the 3D graphics API (e.g., Vulkan, Apple

Metal) and can be viewed almost completely on most medium-high-end smartphones and totally on professional monitors such as the Apple XDR.

To evaluate color patches importance in the CC process and the uniformity of the illumination on the XCC image, we used images coming from a medium format camera equipped with a 100 MP sensor able to acquire 48-bit depth color images and studio lighting. Assessment was performed using these image quality factors calculated using the Imatest Master software [12]:



Fig 1. The target Calibrite ColorChecker Classic.

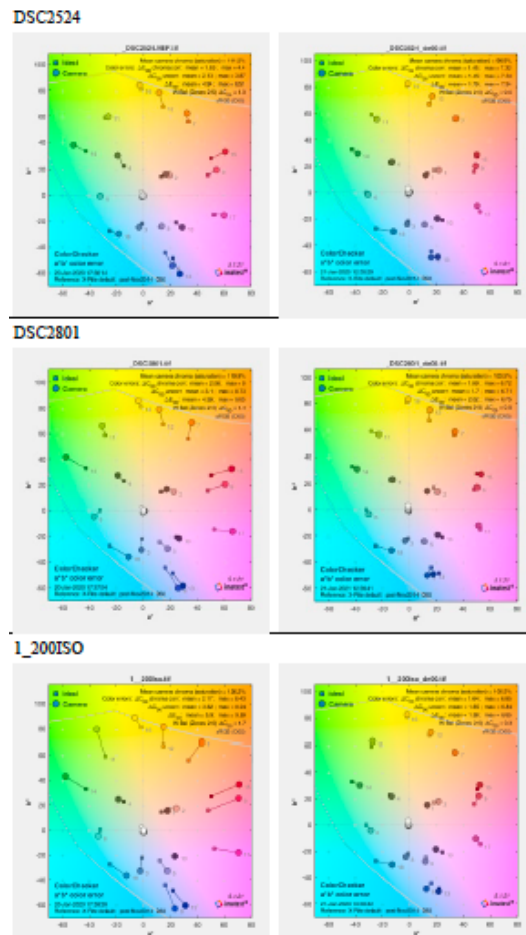


Fig 2. Three images developed through different methods. The first column represents the result of a white balance using the Von Kries white correction. In the second and the third images have been processed through the entire SHAFT development process.

1. ΔE_{00} mean
2. ΔL mean of lightness
3. Exposure error in f-stops measured by pixel levels of patches B4-E4, using gamma values measured rather than the standard value for the color space.

Reference spectral reflectance values come from measurements taken using a spectrophotometer Minolta CM-2600d.

Six class of problems were investigated:

1. Selection of the formula to determine the goodness of the color-correction operation

In evaluating color image capture, it is normally a validation effort aimed at determining goodness of the color-correction operation. This involves comparing the target colorimetry to that predicted from the color profile-processed pixel values.

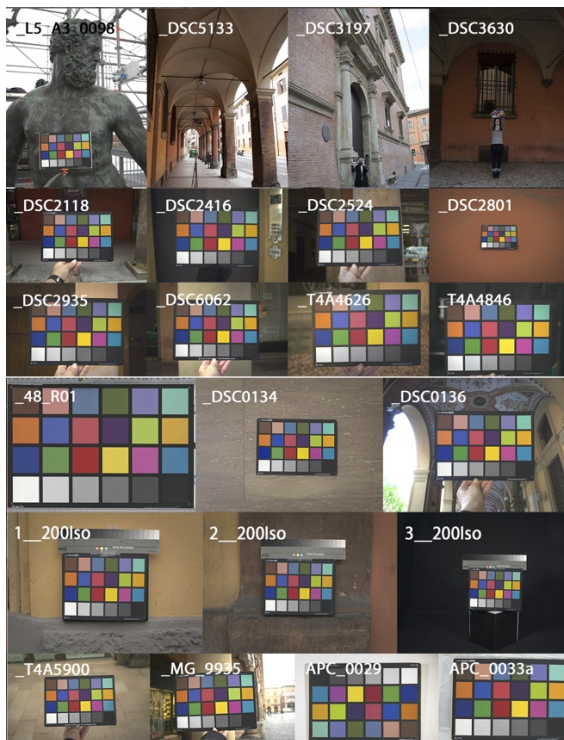


Fig 3. The dataset of 22 RAW images evaluated.

Their use is not limited to the evaluation of the deviation from the desired capture of color image information but is part of a calibration function to establish the best possible mapping from camera RGBs values to device independent XYZs values. Several measurement techniques are used to do this. A commonly used measure is computed as a CIELAB color-difference, ΔE , for each color patch. Usually, the CC technique is then combined with the CIE color metric given by the CIE in 2000 [13]. The formula, even if presents discontinuities, is recommended by CIE mainly for color differences within the range 0–5 of CIELAB units. Many studies focus on the problem of this formula coefficients. However, was demonstrated that the statistical differences reachable are marginal [14] and then the original formulation remains the more easily and reliably usable. Moreover, we compared the CIEDE2000 formula with the Euclidean color-difference formula for small–medium color differences in log-compressed OSA-UCS (Optical Society of America's committee on Uniform Color Scales) space [15,16]. Our attempt is inspired by the study [17], where the UCS diagram based

on CIELUV color space is used to evaluate two color difference formulae ΔE_{00} and ΔE_E for measuring the visual data.

We take the chance to underline that the improvement in precision that follows the choice of the best possible color difference (if it exists) looks negligible comparing the size of differences at the end of the overall process, as the reader can evaluate in the next sessions.

2. Color patches importance in the CC process

As some authors have pointed out, the CC procedure using standard color targets becomes a problem when the object to be reproduced is characterized by colors close to neutral colors [18]. The experimentation of some solutions proposed in the literature (e.g., the construction of tailored chromatic targets with patches empirically chosen within the palette of colors present in the original [19]) has shown a strong uncertainty in the choice of candidate colors, as well as the verification using a different target from the original one has led to disappointing results for the difficulty in reproducing measured color distributions not too dissimilar [20].

A most consistent procedure consists in the assignment of different weights to the different patches of a standard color target. Mainly to emphasize the neutral A4-F4 allow to improve in the scenes with near neutral color, and to assign a higher value the colors closest to the scene allows to improve the quality of reproduction for scene with colors covering only a subset of those reproduced in the color target. Improvement using this solution were tested using different weights (from 0.5 to 4) for the patches B4-E4. Patches A4 and F4 have been excluded to avoid problems related to the saturation and unreliability of their colors.

3. Exposure correctness in the acquired image

One of the main problems affecting image quality, and consequently CC, comes from improper exposure to light. Despite of the great variety of methods for regulating the exposure and the complexity of some of them, it is not rare for images to be acquired with a nonoptimal or incorrect exposure [21]. Under exposure and over exposure have important effects on the spectral response, leading typically to washed out shades. Mostly, such exposure errors are introduced early in the capture process and highly affect the CC results [22]. To evaluate the effect of color alteration due to an incorrect exposition, we exposed the XCC with a series of exposure compensations from -4 EV to +4EV.

4. Uniformity of the illumination

Illuminants are never uniform in real scene and cause interactions and interreflections among objects. To minimize this problem images could be processed using the flat fielding, a post-capture technique aiming to achieve uniform illumination across the image plane and account for differences in pixel photometric sensitivity. Two images are captured: one of the XCC and one of a spatially uniform neutral, e.g., a white paper, that fills the entire field of view. The neutral image captures the distribution of light across the scene. Flat fielding is achieved by dividing the object image by the neutral image and, if required, rescaling, resulting in an image of the scene with uniform illumination. When materials are not perfectly spatially uniform, low-pass spatial filtering, successive imaging and averaging with small displacements of the material, or blurring can be used to minimize the lack of spatial uniformity. We tested images captured under controlled studio lighting system, synthetically deformed to represents different lighting non-uniformity distortions. Cases 0 to 3 reported in Fig. 4 are designed modifying a known and uniform lighting condition (case 0) to increasingly uneven ones. Cases 1 to 3 represent an illumination irregularity ranging from 1 to 4EV measuring exposure in the center and in the margins. Images are evaluated both with and without applying the flat-fielding technique in the [23] implementation.



Fig 4. The synthetically distorted images used to test the flat fielding effects.

5. Noise effects

Among factors determining erroneous results in CC also different types of noise may occur. Image noise is defined in the ISO 15739 standard as “unwanted variations in the response of an imaging system” [24]. It is formed when incoming light is converted from photons to an electrical signal and originates from the camera sensor, its sensitivity, and the exposure time as well as by digital processing (or all these factors together). Noise arises from the effects of basic physics—the photon nature of light and the thermal energy of heat— inside image sensors and amplifiers. The total noise value is a complex mixture of several noise sources of lens system, pixel size, sensor technology and manufacturing, image processing pipeline, ISO speed, exposure time, RAW conversion [25]. Noise scales strongly with pixel size. It can be very low in digital SLRs, which have pixels at least 4 microns square, and it can get problematic in camera phones with tiny sensors, especially at high ISO speeds or in dim light. Noise may cause direct or indirect artifacts to the image. High level of noise values may decrease color accuracy. We tested images synthetically added with different levels of noise ranging from 0 to 25% of pixels. Note that in real case scenarios (e.g., in the images included in the dataset) the maximum amount of noise was recorded across the images taken with a smartphone. According to this scale their amount of noise would have been between 2 and 3%.

6. Glare effects

Among the many sources of noise, a rarely considered factor influencing target-based CC is glare, a systematic departure due to light spread through the lens. Optical veiling glare limits the dynamic range of the image on the sensor and spread on areas differently, in a non-uniform, spatial-dependent way. Its magnitude can be very high, causing big departures from scene values, especially for dark regions [26]. Even if rarely measured, the difference introduced by glare can easily exceed 100 % in the dark areas [27]. Its characteristic is to affect areas differently, according to their mutual spatial distribution. This add a series of local changes that cannot be accounted by a global color Look-Up Table (LUT). In fact, different points in the scene with the same radiance values can easily end up in different acquired values due to different distances from brighter areas in the scene arrangement. This acquisition distortion affects the subsequent CC. A quantitative analysis is conducted comparing a synthetic set of color chart acquisitions. Glare has its paramount effect on the dark areas. It follows that the black patch #24 is the place where glare effect is usually higher. We measured the Glare Evidence (GE) proposed by [28] and defined as follows:

$$GE = \left(\frac{L_B^* \text{acquired}}{L_W^* \text{acquired}} \right) / \left(\frac{L_B^* \text{reference}}{L_W^* \text{reference}} \right)$$

where $L_B \text{acquired}$ and $L_W \text{acquired}$ are the L^* (in $L^*a^*b^*$) derived from the acquired digits and $L_B \text{reference}$ and $L_W \text{reference}$ are the L^*

derived from the actual (contact) measures of the target. L_B refers to the black patches while L_W refers to the white ones.

7. Change of the output color space

The evaluation of the correctness of the CC operation with respect to the output color space is usually omitted, limiting to the consideration that tighter color spaces lead to worse results. We compared the global and per patch means results across different color spaces (the sRGB and the Apple Display P3) in the whole dataset. The IEC 61966-2-1 sRGB, is today the default color space for multimedia application and defined with respect to CIE illuminant D65. It allows consistent color reproduction across different media, the 100% displayability on today's consumer monitors, and full support of 3D API graphics enabling a faithful reproduction of color in 3D applications.

Test results

Here we report the results divided by the 7 points above described.

1. Selection of the formula to determine the goodness of the color-correction operation.

Table 1 and Fig. 5 shows the results of the test. For each image and method, the measurements listed at previous paragraph were performed. The two approaches based on ΔE_{00} and ΔE_E do not show a statistically significant difference.

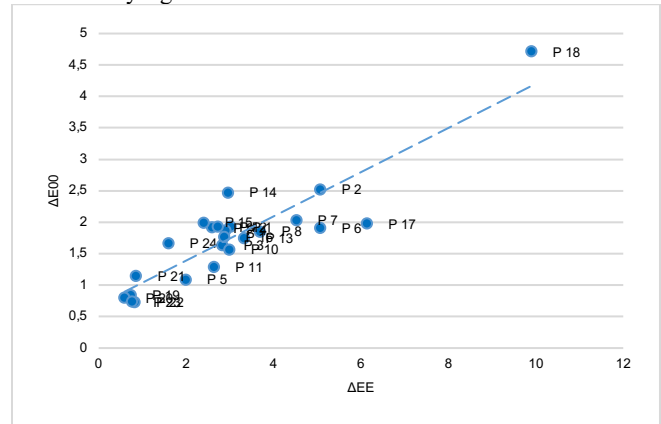


Fig. 5 - Scatterplot of the performance on single patches using the CIEDE2000 and the DEE error metrics. The correlation is noticeable.

2. Color patches importance in the CC process

In Fig. 6 are reported global mean ΔE_{00} values for different weights of the patches B4-E4 in the polynomial fitting of the CC process.

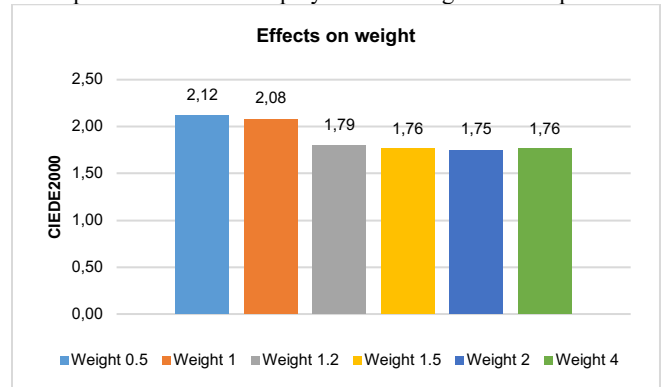


Fig. 6. Global mean ΔE_{00} for different weights of the patches B4-E4 in the polynomial fitting

An improvement of the development performance is already noticeable increasing the weight to 1.2 and the maximum quality is reached at weight 2. Analyzing the color patches error magnitude across the dataset for weight equal 1.2 of patches B4-E4 in the polynomial fitting part of the CC process (Fig. 7), we can see that the error is largely due to patch 18 (F3). The rest of the patches show a rather uniform error, apart from the gray patches, characterized by a lower average error, probably due to the higher weights applied in the weighted polynomial fitting procedure.

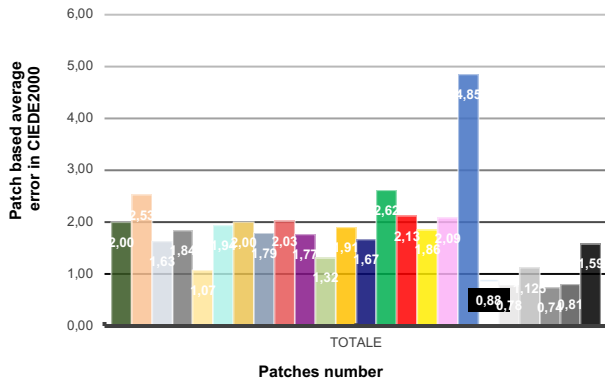


Fig. 7. Color patches error magnitude across the dataset.

3. Exposure correctness in the acquired image

Results of the variation of the exposure compensation are in Fig. 8. Overexposed images (+0.5EV to +4.0EV) are not reported here since they lead to a curve that is symmetrical to the one presented above. The whole dataset has been underexposed from -0.5EV to 4.0EV and the results have been reported above. Note that the ΔE_{00} difference is relatively small (0.11 from -0 EV to -4.0EV).

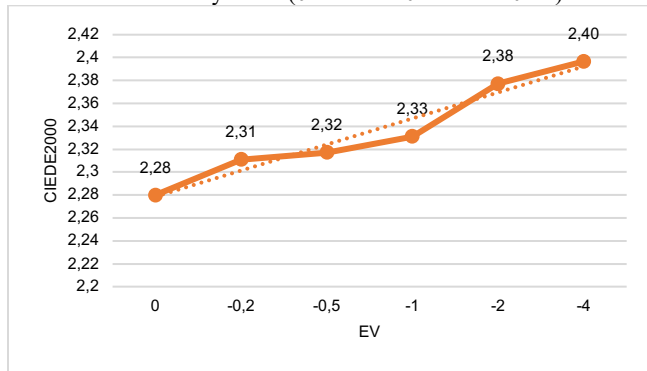


Fig. 8. The effects of exposure on development results.

4. Uniformity of the illumination on the target image

Fig. 9 shows that the illumination irregularity ranging from +1 to +4EV measuring exposure in the center and in the margins determine an exponential degradation of the ΔE_{00} means values. The flat fielding procedure is quite limited in containing the degrading effect of uneven illumination.

5. Noise effects

Fig. 10 shows the variation of ΔE_{00} improving the amount of noise measured as percentage of pixel noised of the whole image. It's possible to note that the ΔE_{00} variation scale linearly. The correlation between the quantity of noise across the experimental dataset,

measured as Imatest Signal to Noise ratio in dB, and ΔE_{00} is extremely low (Fig. 11). This could denote a range of noise in the dataset too small to highlight a correlation or, more probably, that there are other more prominent factors which are influencing ΔE_{00} .

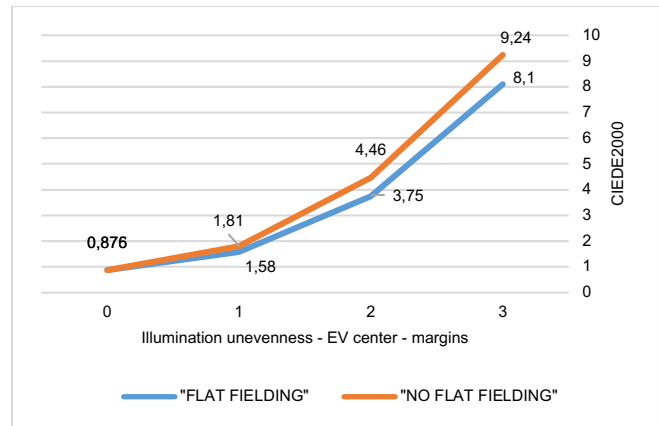


Fig. 9. Effect of lighting non-uniformity distortions on ΔE_{00} means values.

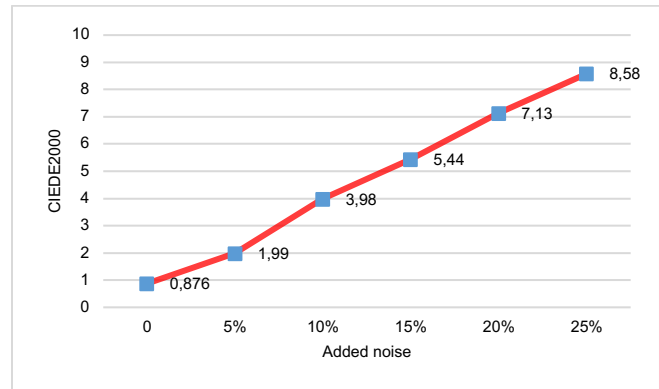


Fig. 10. ΔE_{00} variation increasing the amount of the noise.

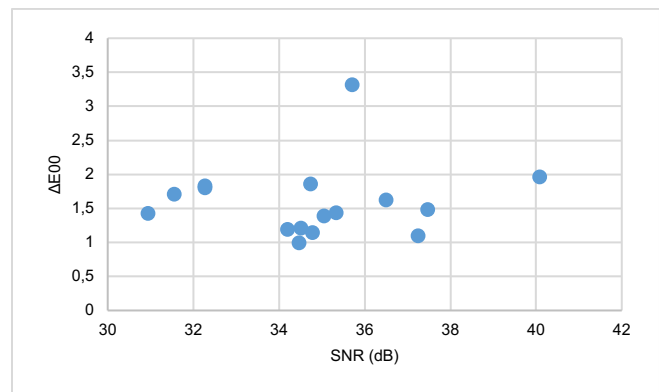


Fig. 11. Correlation between noise and ΔE_{00} across experimental dataset.

6. Glare effects

Table 2 reports the Glare Evidence (GE) showing the glare effect on each target. The reference values are: Black $L^* = 20.64$, White $L^* = 95.17$, B/W Ratio = 0.22. As visible in the last column, the effect of glare on the blacks is paramount. It ranges from a minimum of

58% to a maximum of 169%. It must be considered that glare also affects the other areas, proportionally to their position and ratio with the max luminance in the image [26].

Table 2.

| Image | Acquired Black L* | Acquired White L* | Acquired Ratio B/W | GE Ratio Ac. /Ref. |
|---------|-------------------|-------------------|--------------------|--------------------|
| 48_R01 | 16.96 | 95.09 | 0.18 | 0.82 |
| DSC0134 | 25.59 | 99.77 | 0.26 | 1.18 |
| DSC0136 | 6.27 | 49.45 | 0.13 | 0.58 |
| DSC0945 | 20.65 | 87.78 | 0.24 | 1.08 |
| DSC2118 | 25.01 | 99.74 | 0.25 | 1.16 |
| DSC2416 | 21.76 | 95.69 | 0.23 | 1.05 |
| DSC2524 | 23.23 | 99.34 | 0.23 | 1.08 |
| DSC2801 | 27.38 | 100.00 | 0.27 | 1.26 |
| DSC2935 | 20.67 | 94.81 | 0.22 | 1.01 |
| DSC3197 | 12.07 | 65.29 | 0.18 | 0.85 |
| DSC3630 | 36.58 | 100.00 | 0.37 | 1.69 |
| DSC6062 | 7.83 | 46.96 | 0.17 | 0.77 |
| MG9935 | 18.92 | 87.45 | 0.22 | 1.00 |
| T4A4626 | 7.82 | 52.40 | 0.15 | 0.69 |
| T4A4846 | 16.26 | 97.36 | 0.17 | 0.77 |
| T4A5900 | 19.53 | 91.47 | 0.21 | 0.98 |
| wb_L5A | 24.85 | 98.80 | 0.25 | 1.16 |
| 1_200Is | 23.48 | 98.61 | 0.24 | 1.10 |
| 2_200Is | 25.60 | 100.00 | 0.26 | 1.18 |
| 3_200Is | 25.65 | 100.00 | 0.26 | 1.18 |
| APC0029 | 21.53 | 95.82 | 0.22 | 1.04 |
| APC0033 | 21.41 | 86.03 | 0.25 | 1.15 |

7. Change of the output color space

The chart in Fig. 12 confirms the uniformity in the errors per patch across different color spaces (sRGB and Display-P3) in the whole dataset, showing a strong correlation between patches error.

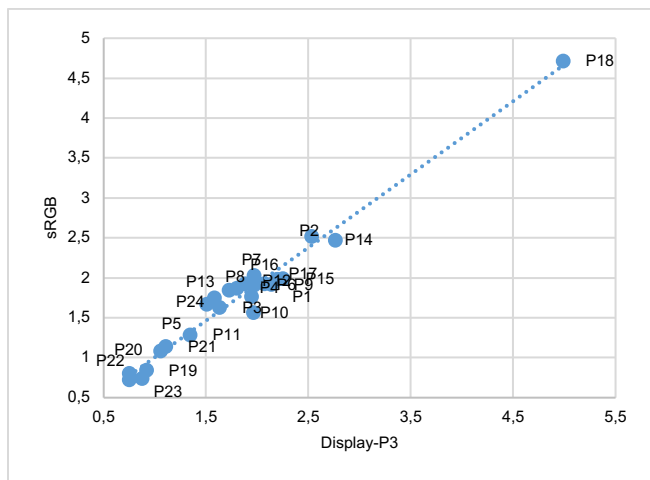


Fig. 12. Patches error correlation in the Display-P3 and sRGB color spaces.

Discussion & conclusions

From previous results we can observe that target-based CC in real scene acquisition is subject to a complex series of color shifts and correction problems that can only aim at lowering these departures, not eliminate them. The type of acquisitions here presented have been realized without any preventative measures, so to be representative of everyday shots.

In such complex scenario it is straightforward that the chosen color difference has a marginal role in the CC process. More extensive analysis about this topic is in a previous paper [29].

Also, the selection of the color space (outside of the specific features of each color space) and the introduction of weights for different patches are factor marginally affecting the results achieved.

Among factors belonging to the real case scenarios noise and exposure, if the CC process is well designed, plays a marginal role. A correlation between the quantity of noise and the resulting *departure* is not noticeable. Underexposures and overexposures of +4.0EV corresponds to growth of the ΔE_{00} of $\cong 0.15$. This could mean that across real world scenarios, or within small ranges of change, causal effects are not the biggest source of departures.

Uneven illumination is a factor presenting a large effect on CC results for values greater than 1EV. The flat fielding technique allows very limited corrections.

Glare has demonstrated to have the larger effect among the tested features, to the point that it makes practically impossible to acquire correctly all the colors in an image [26, 29]. We recall that glare is present in every acquisition device that uses lenses. It scales quickly to values higher than 1 and not is possible any efficient correction.

Concluding we can summarize that an idealized colorimetric correction is far from the acquisition non-linearities common in real acquisitions. From the reported acquisition data, it has been shown the effect of real scene complexity and how colors are subject to disordered shifts in the color space. All the factors considered (error metrics, exposure, illumination uniformity, glare, noise, color space) influence the development process and digit departures from actual scene values shows a progressive increase as the ideal conditions decline. In this process illumination non uniformity and glare play the major role.

The overall sum of all the points influencing acquisition correctness led to departure values of higher order of magnitude compared to the one derived from the fine tuning of each one of them.

References

1. Standardization, I.O.F. Graphic Technology and Photography - Colour Characterisation of Digital Still Cameras (DSCs). ISO 17321-1: 2012, November.
2. Colantoni P, Thomas JB, Hardeberg JY. High-end colorimetric display characterization using an adaptive training set. J. Soc. Inf. Disp. 2011; 19: 520-530.
3. <https://www.xrite.com/categories/calibration-profiling/colorchecker-classic>.
4. Reinhard, E., Arif Khan, E., Oguz Akyuz, A., Johnson, G., 2008. Color Imaging Fundamentals and Applications. A. K. Peters/CRC Press, Boca Raton.
5. J.J. McCann, and A. Rizzi, The Art and Science of HDR Imaging, (John Wiley, 2011).
6. K. Borrino, F.V. de Azambuja, N. Sampat, and J.A.S. Viggiano, "Sensitivity analysis applied to ISO recommended camera color calibration methods to determine how much of an advantage, if any, does spectral characterization of the camera offer over the chart-based approach", in Electronic Imaging, Digital Photography and Mobile Imaging XIII (2017), pp. 32-36.
7. M. Gaiani, and A. Ballabeni, "SHAFT (SAT & HUE Adaptive Fine Tuning), a new automated solution for target-based color correction", in Colour and Colorimetry Multidisciplinary Contributions (2018), **XIVB**, pp. 69-80.
8. <https://www.libraw.org/>.
9. E.-S. Kim, S.-H. Lee, S.-W. Jang, and K.-I. Sohng, "Adaptive colorimetric characterization of camera for the variation of white balance," IEICE Trans. on Electronics, **E88-C** (11), 2086-2089 (2005).

10. M. Gaiani, F.I. Apollonio, A. Ballabeni, and F. Remondino, "Securing Color Fidelity in 3D Architectural Heritage Scenarios", *Sensors* **17**(11), 2437-1-2437-24 (2017).
11. Stokes, M., Anderson, M., Chandrasekar, S., Motta, R., 1996. A Standard Default Color Space for the Internet – sRGB. <http://www.w3.org/Graphics/Color/sRGB>.
12. Imatest, <https://www.imatest.com>.
13. Colorimetry–Part 6: CIEDE2000 Colour-Difference Formula", ISO/CIE 11664-6: 2014.
14. Melgosa, M. et. al. (2017) 'Revisiting the weighting function for lightness in the CIEDE2000 colour-difference formula', *Col. Technol.*, 133(4), pp. 273-282.
15. C. Oleari, M. Melgosa, and R. Huertas, "Euclidean color-difference formula for small-medium color differences in log-compressed OSA-UCS space", *J. Opt. Soc. Am. A*, **26**(1), 121-134 (2009).
16. M. Melgosa, D. Pant, G. Simone, "Revisiting the Optical Society of America Uniform Color Scales system: past, present and future challenges", *Col. Technol.* **137**(1), 33-37 (2021).
17. D.R. Pant, and I. Farup, "CIE uniform chromaticity scale diagram for measuring performance of OSA-UCS ΔE and CIEDE00 formulas", in 3rd European Workshop on Visual Information Processing (2011), pp. 18-23.
18. Berns, R. S., Taplin, L. A., Nezamabadi, M., Zhao, Y., and Okumura, Y. (2005) 'High-Accuracy Digital Imaging of Cultural Heritage without Visual Editing', in Proceedings of IS&T Archiving Conference, pp. 91-95
19. Williams, D. and Burns, P. D. (2012) 'Targeting for Important Color Content: Near Neutrals and Pastels', in Proceedings of IS&T Archiving 2012 Conference, pp. 190-194.
20. Williams, D. and Burns, P. D. (2016) 'Color Correction Meets Blind Validation for Image Capture: Are We Teaching to the Test?', in Proceedings of IS&T International Symposium on Electronic Imaging, pp. 218.1-218.4.
21. Hazem Wannous, Yves Lucas, Sylvie Treuillet, Alamin Mansouri, Yvon Voisin. Improving color correction across camera and illumination changes by contextual sample selection. *Journal of Electronic Imaging, SPIE and IS&T*, 2012, 21 (2), pp.023015-1–023015-14. 10.1117/1.JEI.21.2.023015. hal- 00719790]
22. Hakki Can Karaimer and Michael S Brown. A software platform for manipulating the camera imaging pipeline. In ECCV, 2016.
23. J. Witwer, and R. Berns, "Increasing the Versatility of Digitizations through Post-Camera Flat-Fielding", in Proceedings of IS&T Archiving Conference (2015), pp. 110-113.
24. ISO 15739: 2013 Photography—Electronic Still-Picture Imaging—Noise Measurements. 2013. Available online: http://www.iso.org/iso/home/store/catalogue_ics/catalogue_detail_ics.htm?csnumber=59420 (accessed on 10 March 2019).
25. Peltoketo, V.-T., 2015. SNR and Visual Noise of Mobile Phone Cameras. *Journal of Imaging Science and Technology*, 59(1), 10401-1-10401-7(7))
26. J.J. McCann, V. Vonikakis, and A. Rizzi, HDR Scene Capture and Appearance, (SPIE, 2017).
27. J. McCann, ColorChecker at the beach: dangers of sunburn and glare Proc. SPIE 9015, Color Imaging XIX: Displaying, Processing, Hardcopy, and Applications, 90150V (2014); doi:10.1117/12.2045379.
28. A. Signoroni, M. Conte, A. Plutino, and A. Rizzi, "Spatial-Spectral Evidence of Glare Influence on Hyperspectral Acquisitions", *Sensors*, **20**, 4374 (2020).
29. Gabriele Simone, Marco Gaiani, Andrea Ballabeni, and Alessandro Rizzi, "Complex process of image color correction: a test of a target-based framework," *J. Opt. Soc. Am. A* **38**, 663-674 (2021)

Table 1. Test results of the optimization process experimented (ΔE_{00} -based and ΔE_E -based) using the dataset in fig. 2.

| Image id | ΔE_{00} | | | | | | | ΔE_E | | | | | | |
|-------------|-----------------|-------------|-----------------|--------------|----------------|-----------------|------------------|-----------------|-------------|-----------------|--------------|----------------|-----------------|------------------|
| | ΔE_{00} | ΔL | $\Delta Chroma$ | ΔHue | Exposure error | Processing Time | Number of cycles | ΔE_{00} | ΔL | $\Delta Chroma$ | ΔHue | Exposure error | Processing Time | Number of cycles |
| 48_R01 | 2.93 | 1.36 | 3.58 | 2.68 | 0.17 | 162.00 | 125 | 3.33 | 1.16 | 4.11 | 3.31 | 0.17 | 158.00 | 125 |
| DSC0134 | 2.17 | 1.27 | 2.16 | 1.58 | 0.08 | 31.25 | 125 | 2.31 | 1.09 | 1.76 | 2.05 | 0.08 | 35.01 | 125 |
| DSC0136 | 2.57 | 1.21 | 2.96 | 2.38 | 0.08 | 32.29 | 110 | 3.41 | 1.12 | 3.19 | 3.73 | 0.08 | 36.07 | 125 |
| DSC0945 | 4.39 | 2.79 | 5.12 | 3.15 | 0.18 | 51.00 | 125 | 5.23 | 2.73 | 5.48 | 4.31 | 0.18 | 51.01 | 30 |
| DSC2118 | 2.32 | 1.53 | 2.05 | 1.95 | 0.04 | 38.86 | 125 | 2.68 | 1.29 | 1.82 | 2.58 | 0.03 | 40.04 | 125 |
| DSC2416 | 2.70 | 1.50 | 3.03 | 2.21 | 0.10 | 37.64 | 220 | 2.85 | 1.30 | 3.80 | 2.53 | 0.10 | 36.08 | 315 |
| DSC2524 | 1.80 | 0.94 | 2.11 | 1.62 | 0.06 | 36.05 | 125 | 2.04 | 0.80 | 2.20 | 2.10 | 0.06 | 40.14 | 125 |
| DSC2801 | 2.01 | 0.98 | 1.98 | 2.02 | 0.06 | 37.40 | 220 | 2.38 | 0.73 | 2.15 | 2.76 | 0.06 | 40.41 | 220 |
| DSC2935 | 3.60 | 2.36 | 3.78 | 2.43 | 0.10 | 39.44 | 126 | 3.71 | 2.13 | 4.47 | 2.73 | 0.11 | 39.71 | 125 |
| DSC3197 | 2.51 | 1.59 | 2.08 | 2.18 | 0.07 | 33.21 | 505 | 5.47 | 3.62 | 4.82 | 5.43 | 0.07 | 34.24 | 410 |
| DSC3630 | 2.30 | 1.26 | 2.04 | 2.07 | 0.09 | 35.28 | 505 | 2.98 | 1.54 | 2.81 | 2.74 | 0.09 | 34.76 | 410 |
| DSC6062 | 2.35 | 1.62 | 2.81 | 1.66 | 0.15 | 37.84 | 30 | 2.84 | 1.45 | 2.91 | 2.47 | 0.15 | 40.16 | 220 |
| MG9935 | 2.60 | 1.64 | 2.97 | 1.82 | 0.08 | 42.01 | 30 | 3.26 | 1.74 | 3.55 | 2.67 | 0.08 | 44.71 | 125 |
| T4A4626 | 4.69 | 4.15 | 3.50 | 2.56 | 0.08 | 47.48 | 30 | 5.11 | 4.00 | 3.62 | 4.02 | 0.08 | 49.92 | 125 |
| T4A4846 | 2.36 | 1.20 | 3.16 | 2.03 | 0.11 | 48.18 | 125 | 5.11 | 4.00 | 3.62 | 4.02 | 0.08 | 50.48 | 31 |
| T4A5900 | 2.73 | 1.26 | 3.23 | 2.42 | 0.11 | 45.27 | 220 | 3.00 | 1.41 | 2.83 | 2.89 | 0.06 | 48.49 | 125 |
| wb_L5_A | 2.33 | 1.32 | 2.42 | 1.97 | 0.08 | 48.00 | 200 | 3.00 | 1.10 | 2.36 | 3.18 | 0.08 | 48.00 | 200 |
| 1_200ls | 1.98 | 0.96 | 2.23 | 1.86 | 0.08 | 50.00 | 125 | 2.24 | 0.69 | 2.00 | 2.47 | 0.08 | 52.44 | 125 |
| 2_200ls | 2.46 | 1.24 | 3.91 | 2.11 | 0.08 | 50.73 | 31 | 2.84 | 1.02 | 3.95 | 2.69 | 0.08 | 53.39 | 126 |
| 3_200ls | 2.20 | 1.16 | 2.29 | 1.72 | 0.09 | 50.11 | 30 | 2.78 | 0.70 | 2.03 | 3.12 | 0.09 | 50.01 | 125 |
| APC0029 | 3.70 | 2.20 | 5.09 | 2.60 | 0.14 | 35.13 | 126 | 3.86 | 2.17 | 5.54 | 2.61 | 0.14 | 36.32 | 125 |
| APC0033 | 5.42 | 3.39 | 6.34 | 3.97 | 0.19 | 31.45 | 315 | 5.93 | 3.21 | 7.11 | 4.68 | 0.18 | 37.69 | 220 |
| Mean | 2.82 | 1.68 | 3.15 | 2.24 | 0.10 | 46.39 | 162.41 | 3.47 | 1.77 | 3.51 | 3.19 | 0.10 | 48.05 | 167.36 |